An adaptive planning strategy for station parameter optimized radiation therapy (SPORT): Segmentally boosted VMAT

Ruijiang Li and Lei Xing

Articles you may be interested in

Automatic CT simulation optimization for radiation therapy: A general strategy
Med. Phys. **41**, 031913 (2014); 10.1118/1.4866377

Optimization of normalized prescription isodose selection for stereotactic body radiation therapy: Conventional vs robotic linac
Med. Phys. **40**, 051705 (2013); 10.1118/1.4798944

Accurate description of heterogeneous tumors for biologically optimized radiation therapy
Med. Phys. **32**, 1825 (2005); 10.1118/1.1924310

Penalized likelihood fluence optimization with evolutionary components for intensity modulated radiation therapy treatment planning
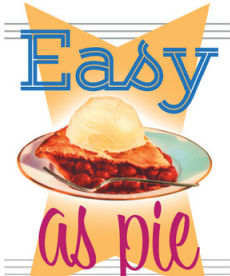Med. Phys. **31**, 2335 (2004); 10.1118/1.1773631

Beyond bixels: Generalizing the optimization parameters for intensity modulated radiation therapy
Med. Phys. **29**, 2298 (2002); 10.1118/1.1508799

Medical Physics Letter

An adaptive planning strategy for station parameter optimized radiation therapy (SPORT): Segmentally boosted VMAT

Ruijiang Li and Lei Xing[a)]
Department of Radiation Oncology, Stanford University, Stanford, California 94305-5847

Purpose: Conventional volumetric modulated arc therapy (VMAT) discretizes the angular space into equally spaced control points during planning and then optimizes the apertures and weights of the control points. The aperture at an angle in between two control points is obtained through interpolation. This approach tacitly ignores the differential need for intensity modulation of different angles. As such, multiple arcs are often required, which may oversample some angle(s) and undersample others. The purpose of this work is to develop a segmentally boosted VMAT scheme to eliminate the need for multiple arcs in VMAT treatment with improved dose distribution and/or delivery efficiency.

Methods: The essence of the new treatment scheme is how to identify the need of individual angles for intensity modulation and to provide the necessary beam intensity modulation for those beam angles that need it. We introduce a "demand metric" at each control point to decide which station or control points need intensity modulation. To boost the modulation at selected stations, additional segments are added in the vicinity of the selected stations. The added segments are then optimized together with the original set of station or control points as a whole. The authors apply the segmentally boosted planning technique to four previously treated clinical cases: two head and neck (HN) cases, one prostate case, and one liver case. The proposed planning technique is compared with conventional one-arc and two-arc VMAT.

Results: The proposed segmentally boosted VMAT technique achieves better critical structure sparing than one-arc VMAT with similar or better target coverage in all four clinical cases. The segmentally boosted VMAT also outperforms two-arc VMAT for the two complicated HN cases, yet with ∼30% reduction in the machine monitor units (MUs) relative to two-arc VMAT, which leads to less leakage/scatter dose to the patient and can potentially translate into faster dose delivery. For the less challenging prostate and liver cases, similar critical structure sparing as the two-arc VMAT plans was obtained using the segmentally boosted VMAT. The benefit for the two simpler cases is the reduction of MUs and improvement of treatment delivery efficiency.

Conclusions: Segmentally boosted VMAT achieves better dose conformality and/or reduced MUs through effective consideration of the need of individual beam angles for intensity modulation. Elimination of the need for multiple arcs in rotational arc therapy while improving the dose distribution should lead to improved workflow and treatment efficacy, thus may have significant implication to radiation oncology practice. © *2013 American Association of Physicists in Medicine.* [http://dx.doi.org/10.1118/1.4802748]

I. INTRODUCTION

The quality of radiation therapy (RT) treatment depends critically on the available degree of freedom of the delivery system.[1] With the introduction of intensity modulated radiation therapy (IMRT) and volumetric modulated arc therapy (VMAT) through the development of dynamic MLC delivery techniques, the landscape of RT practice has changed dramatically in the past two decades. For historical reasons, the beam angular sampling and the modulation of individual beams in current IMRT and VMAT are treated as two independent groups of variables with the interplay between them ignored tacitly during the plan optimization. Conventional IMRT (with 5–10 beams), for example, often does not possess sufficient angular sampling required to spatially spread the dose. On the contrary, current VMAT (with 1–3 arcs) may under- or overmodulate in some or all directions. The concept of dense angularly sampled and sparse intensity modulated radiation therapy (DISSAM-RT), which can be achieved by increasing the angular beam sampling while eliminating dispensable segments of the incident fields,[2] has been introduced to optimally explore a large area of uncharted territory in terms of the number of beams (including noncoplanar and/or nonisocentric beams) and beam modulation. Furthermore, in a recent Point and Counterpoint discussion,[3] we have pointed out that the most general implementation of DASSIM-RT can

be described as station parameter optimized radiation therapy (SPORT) in the new age of digital RT. Briefly, a station control point (or node or control point) describes the state of delivery system (including LINAC configurations such as beam energy, aperture shape and weight, gantry/collimator angle,[4] and auxiliaries such as the couch). When the auxiliary equipment is stationary, a station control point is not different from a MLC or jaw-shaped beam. A conventional intensity-modulated beam consists of a collection of stations with the same gantry angle but different MLC settings. VMAT and IMRT are simply two special, and often nonoptimal, cases of SPORT.

Deliverywise, a number of variants of SPORT are possible. Here, we present a rotational arc strategy in which the traditional one-arc VMAT is differentially boosted by inserting additional modulated apertures on an on-demand basis. The insertions of additional apertures differentially "boost" the original treatment plan so that target coverage is improved while sparing the sensitive structures. Because of the selective nature of the angular boost, the proposed planning scheme rivals the conventional multiple arc treatment—it often outperforms the multiple-arc VMAT plan while shortening the delivery time, leading to a simplified and efficient treatment.

II. METHODS AND MATERIALS

For a given case, the demand for intensity modulation varies from angle to angle in a rotational arc delivery. The essence of SPORT planning is how to identify the need of individual angles for intensity modulation and to provide the necessary beam intensity modulation for those beam angles that need it. We plan the segmented boost treatment in an adaptive fashion by starting from an optimized one-arc VMAT. The angles that need a higher level of intensity modulation are identified with the help of a newly introduced "demand metric." Additional segments are then added in the vicinity of the angles that require high intensity modulation. The modified arc plan of the original one-arc VMAT with the added segments is reoptimized as a whole to provide the final segmented boost VMAT treatment plan. Figure 1 shows a schematic plot of the beam angular distributions of conventional VMAT and segmentally boosted VMAT.

II.A. Treatment planning

A clinical Eclipse™ treatment planning system (Varian Medical Systems, Palo Alto, CA) is used for the implementation of the proposed SPORT treatment scheme. We first obtain an one-arc VMAT treatment plan using the system with 178 station control points uniformly distributed in the range of 0°–360°. There are several ways to determine which directions need additional segmental boost. We examine the degree of segmental modulation around each station control point and then place more segments around the control points with higher modulations as, intuitively, adding segment(s) to these station control points would be more beneficial for improved dose distribution. To quantify the level of intensity modulation of a station point, we introduce a demand metric called
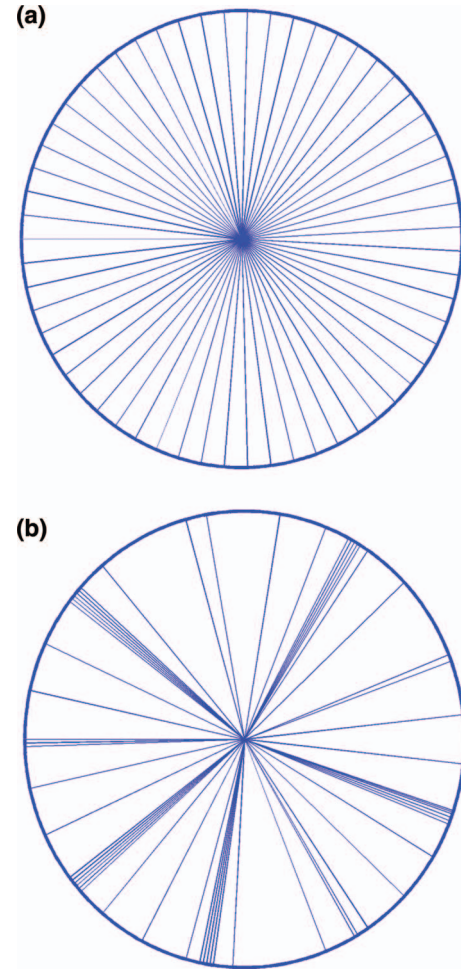

FIG. 1. Schematic plot of the beam angular distributions for two treatment schemes: (a) conventional VMAT and (b) proposed SPORT. The lines indicate the gantry angles of the station points or control points.

modulation index (MI) as follows:

$$\mathrm{MI}(s) = \sum_{\substack{k=-K\ldots \\ K, k \neq 0}} \left[\sum_{i=1}^{60} \left(\left| x_i^A(s) - x_i^A(s+k) \right| + \left| x_i^B(s) - x_i^B(s+k) \right| \right) \right] \cdot \left| \frac{\mathrm{MU}(s) - \mathrm{MU}(s+k)}{\alpha(s) - \alpha(s+k)} \right|,$$

(1)

where $x_i^A(s)$ and $x_i^B(s)$ are the ith MLC leaf positions at banks A and B at the sth station control point, MU is the cumulative monitor units, α is the gantry angle. Intuitively, MI is the local geometric modulation weighted by the corresponding segmental MU per gantry angle. In this work, the neighboring $2K$ station control points ($K = 10$ in this study) are used to calculate the MI of a station point.

To differentially boost the individual angles with high MI values, we add a certain number of small arcs (spanning $\sim 30°$) around the selected station points. The original one-arc VMAT with the added partial arcs are then optimized as a whole by using the same treatment planning system.

We apply the proposed planning technique to four previously treated clinical cases: two head and neck (HN) cases,

one prostate, and one liver case. For HN case 1, a total dose of 70 Gy was prescribed to the planning target volume (PTV) over 35 fractions. For HN case 2, there are two PTV targets: one was prescribed to a total dose of 66 Gy, and the other was prescribed to a total dose of 54 Gy in 30 fractions. For the prostate patient, a total dose of 78 Gy was prescribed to the PTV over 39 fractions. For the liver patient, a total dose of 60 Gy was prescribed to the PTV over 30 fractions. 6 MV photons were chosen for the HN cases, and 15 MV photons were chosen for the prostate and liver cases. For comparison purpose, conventional VMAT plans with one and two full arcs across the 0°–360° angular space are also generated for the four cases. All treatment plans were normalized in such a way that 95% of the PTV receives the prescribed dose.

II.B. Plan evaluation

We demonstrate the quality of the resultant treatment plans using dose volume histogram (DVH) and isodose distributions. We also calculated the equivalent uniform dose[5–7] (EUD) for both target and organs at risk, which is defined as: $\text{EUD} = \left(\frac{1}{n}\sum_{i=0}^{n} d_i^a\right)^{1/a}$, where d_i is the dose received by voxel i, and n is the total number of voxels in the region of interest. In calculating EUD, we chose the values for parameter a to be −10, 1, and 6 for the tumor target, parallel organs (such as parotid glands), and serial organs (such as spinal cord), respectively.

III. RESULTS

Figure 2 shows the MI as a function of gantry angle for HN case 1, after a conventional VMAT plan is optimized with uniformly distributed control points. As can be seen, there are clearly three distinct local maxima centering around roughly 40°, 135°, and 235°. Three small arcs (each span-
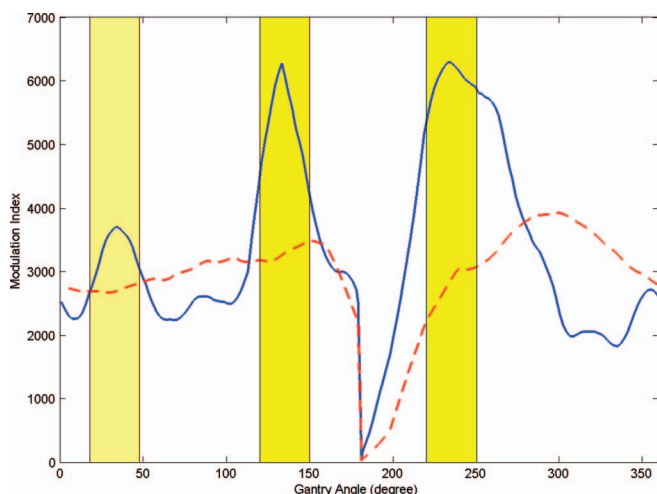

FIG. 2. Modulation index (solid) as a function of gantry angle for the HN case 1, after an initial VMAT treatment plan is optimized with uniformly distributed control points. Three arcs (shown in shaded areas) are added to the initial one-arc VMAT plan. The dashed line indicates the modulation index for the updated one-arc VMAT plan after the combined system is optimized. The modulation index significantly decreases at those gantry angles with boosted segments.
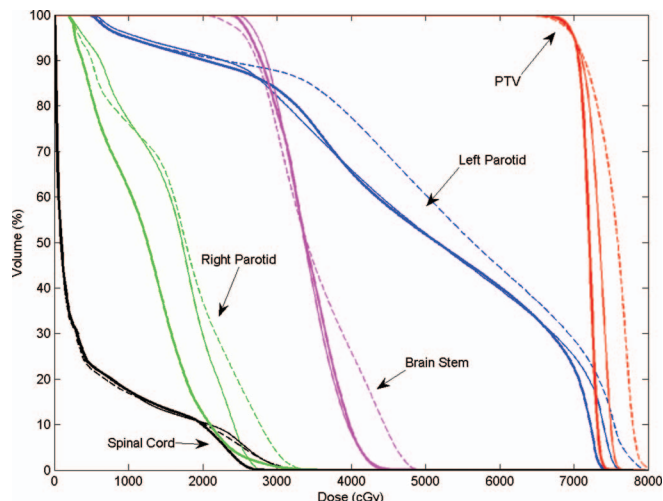
FIG. 3. DVHs of three different treatment plans: one-arc VMAT (dashed line), two-arc VMAT (solid thin), and segment boosted VMAT (solid thick) for HN case 1.

ning ∼30° around one local maximum) are then added to the initial VMAT plan and the combined system is optimized as a whole. The MI for the updated plan (dashed line in Fig. 2) significantly decreases at those gantry angles with boosted segments, indicating that the need for intensity modulation has been partially met by the added or boosted segments.

Figures 3–6 show the DVHs of three different treatment plans for the four clinical cases. For HN case 1 (Fig. 3), it can be seen that segmentally boosted VMAT clearly improves both one-arc and two-arc VMAT, in terms of target coverage and critical structure sparing. For the more complicated HN case 2 (Fig. 4), with similar target coverage, our technique also achieves better critical structure sparing, particularly for left parotid, spinal cord, and chiasm. In the liver and prostate cases (Figs. 5 and 6), the segmentally boosted VMAT far outperforms one-arc VMAT in terms of critical structure sparing, and achieves a similar or better plan quality with that of two-arc VMAT. For instance, the technique improves
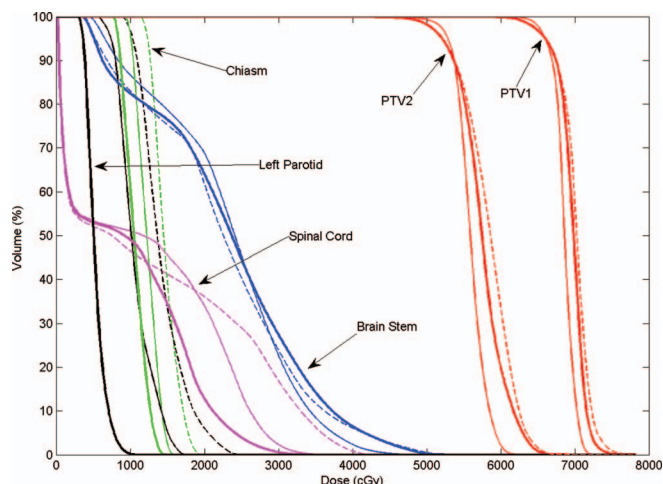

FIG. 4. DVHs of three different treatment plans: one-arc VMAT (dashed line), two-arc VMAT (solid thin), and segment boosted VMAT (solid thick) for HN case 2.

FIG. 5. DVHs of three different treatment plans: one-arc VMAT (dashed line), two-arc VMAT (solid thin), and segment boosted VMAT (solid thick) for the liver case.
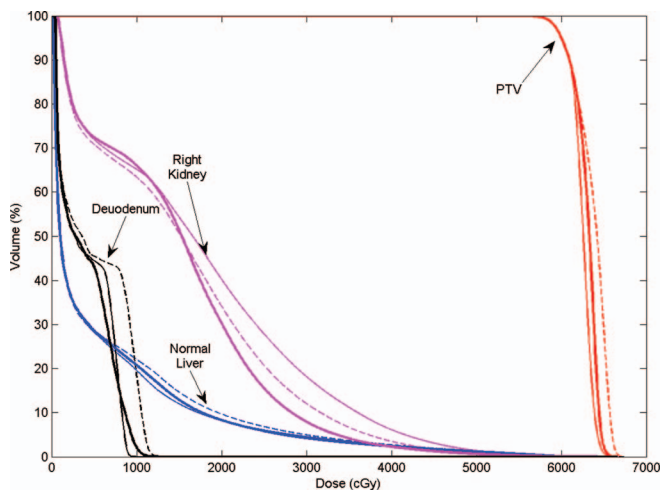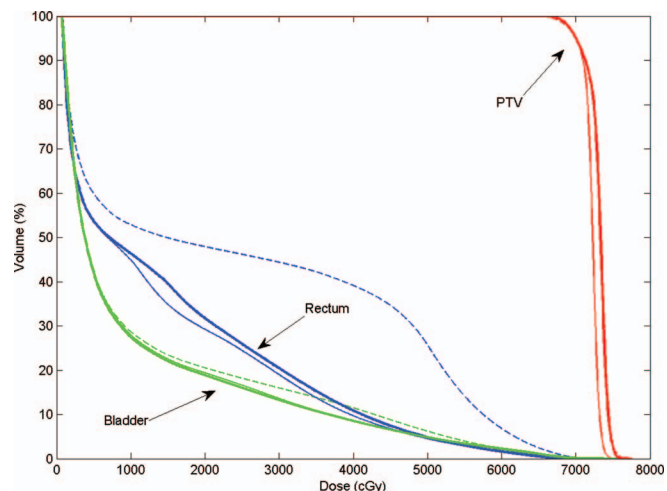
FIG. 6. DVHs of three different treatment plans: one-arc VMAT (dashed line), two-arc VMAT (solid thin), and segment boosted VMAT (solid thick) for the prostate case.

FIG. 7. Axial (top row), coronal (mid row), and sagittal (bottom row) views of the isodose distributions for three treatment plans: one-arc VMAT (left column), 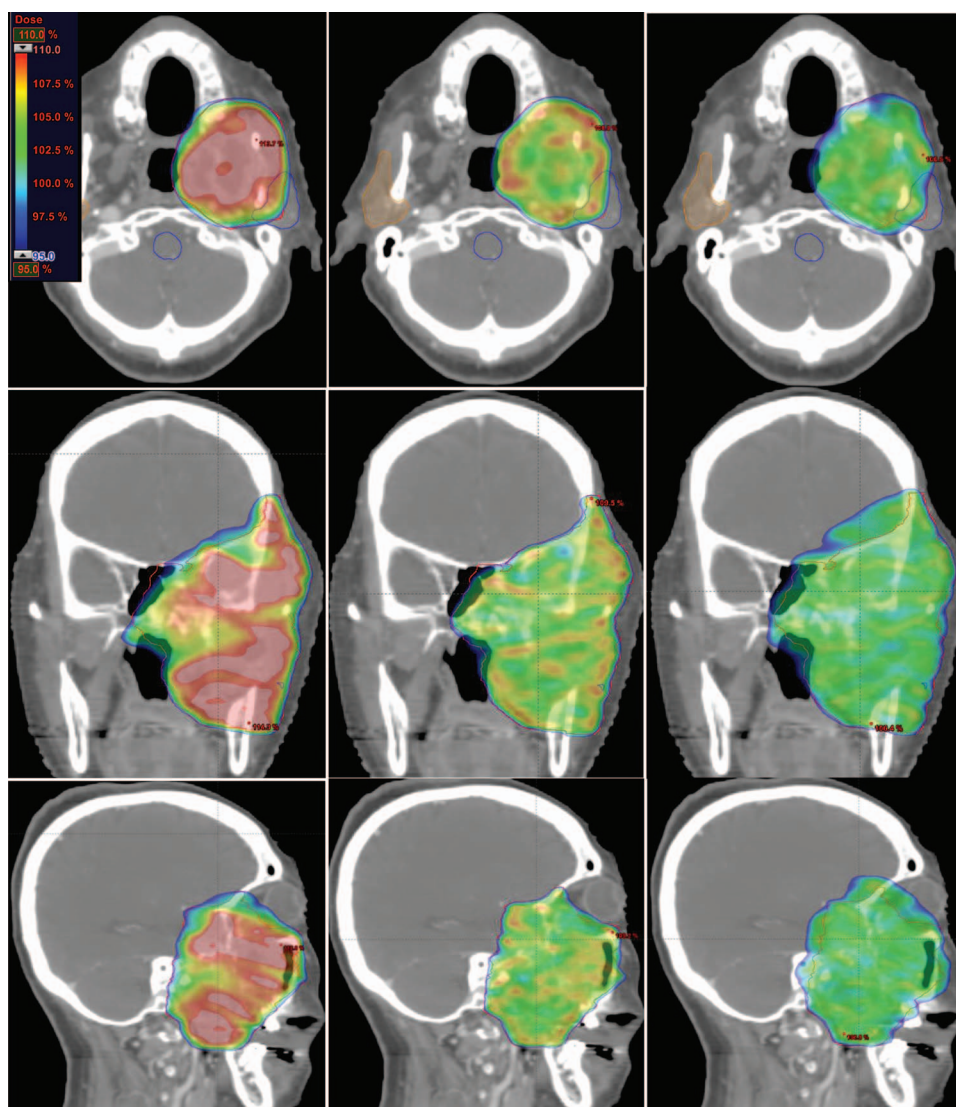two-arc VMAT (mid column), and segment boosted VMAT (right column) at a dose level of 95%–110% for HN case 1. Segment boosted VMAT achieves more uniform target coverage.

TABLE I. Equivalent uniform dose and MU in four clinical cases for one-arc, two-arc, and segmentally boosted VMAT plans.

Patient	EUD (MU)	One-arc VMAT	Two-arc VMAT	Segmentally boosted
Head and neck 1: 70 Gy in 35 fractions	PTV	74.6	72.9	71.8
	Brain stem	37.7	35.1	**35.0**[a]
	Spinal cord	18.2	18.3	**16.2**[a]
	Parotid (left)	53.5	50.0	**49.4**[a]
	Parotid (right)	17.0	16.0	**12.3**[a]
	MU	276	520	360
Head and neck 2: 66 Gy to PTV1, 54 Gy to PTV2 in 30 fractions	PTV1	69.5	68.4	69.2
	PTV2	56.8	55.5	56.3
	Brain stem	31.3	**29.1**[a]	31.6
	Chiasm	14.7	12.2	**10.6**[a]
	Spinal cord	26.9	21.7	**18.3**[a]
	Parotid (left)	14.2	10.5	**5.2**[a]
	MU	352	488	382
Liver: 60 Gy in 30 fractions	PTV	63.3	62.3	62.7
	Normal liver	6.2	5.8	**5.8**[a]
	Duodenum	8.7	**6.8**[a]	7.0
	Kidney (right)	15.5	17.3	**14.9**[a]
	MU	375	638	450
Prostate: 78 Gy in 39 fractions	PTV	81.2	80.2	81.2
	Rectum	52.8	**41.1**[a]	41.5
	Bladder	42.7	**41.9**[a]	42.0
	MU	342	454	413

[a]Bold numbers indicate the smallest EUD for critical structures among the three plans.

significantly the dose to the right kidney. With only one boost from around the AP direction, the dose to rectum in the prostate case was significantly reduced compared with one-arc VMAT. The EUDs of the targets and critical structures for different plans (Table I) reveal the same pattern for all clinical cases studied here. Furthermore, we found that the proposed treatment scheme generally leads to more uniform target dose. For instance, using the definition of uniformity index: UI $= D_5/D_{95}$, where D_5 and D_{95} are the minimum doses delivered to 5% and 95% of the PTV,[8] the target uniformity index in HN case 1 is 1.12, 1.08, and 1.05 for one-arc, two-arc, and segmentally boosted VMAT (the closer this number is to unity, the more uniform the dose distribution is).

To better illustrate the advantage of segmentally boosted VMAT, Figs. 7–9 show the isodose distributions of the three treatment plans for HN case 1. At the highest dose level (>95% of prescription dose), segmentally boosted VMAT achieves better target dose uniformity. One-arc VMAT plan gives a maximum point dose as high as 116%. At medium and low dose levels, segmentally boosted VMAT has better sparing of brain stem and right parotid than one-arc and/or two-arc VMAT. Better critical sparing with segmentally boosted VMAT is also observed in HN case 2 (Figs. 10 and 11).

IV. DISCUSSION

In current VMAT optimization methods, the angular space is divided into equally spaced control points and the corresponding weights and apertures of the incident beams are then optimized. The field in between two adjacent station control points is derived by linear interpolation of the parameters of the two adjacent points. This approach is inherently nonoptimal and, depending on the size of the angular discretization, some directions may be under- or overmodulated. This is why one-arc VMAT generally does not offer sufficient beam modulation for many cases and two or multiple arcs are often required.

In reality, the angular need for intensity modulation is not uniform. Depending on the patient, some angles require more modulation than others. This work presents a novel rotational arc therapy strategy with selective angular sampling of control points guided by the actual need of individual gantry angles. Intellectually, this is the first time that differential angular sampling is formally formulated and algorithmically implemented. Being able to replace the existing multiple arcs VMAT by a single rotation, yet with better dose distribution and reduced MUs, represents a major leap in the field and may have significant implications in improving the current workflow and patient care. While the proposed scheme is conceptually a special case of SPORT that has been discussed in a previous publication, the novel rotational arc planning and delivery and algorithmic details (such as the introduction of a demand metric and the adaptive nonuniform sampling strategy of the control points) are essential to the actual rotational arc realization of the general SPORT concept. Dramatically different from simply increasing the number of arcs for VMAT or beams for IMRT, the dosimetric improvement in our approach is achieved by considering the interplay
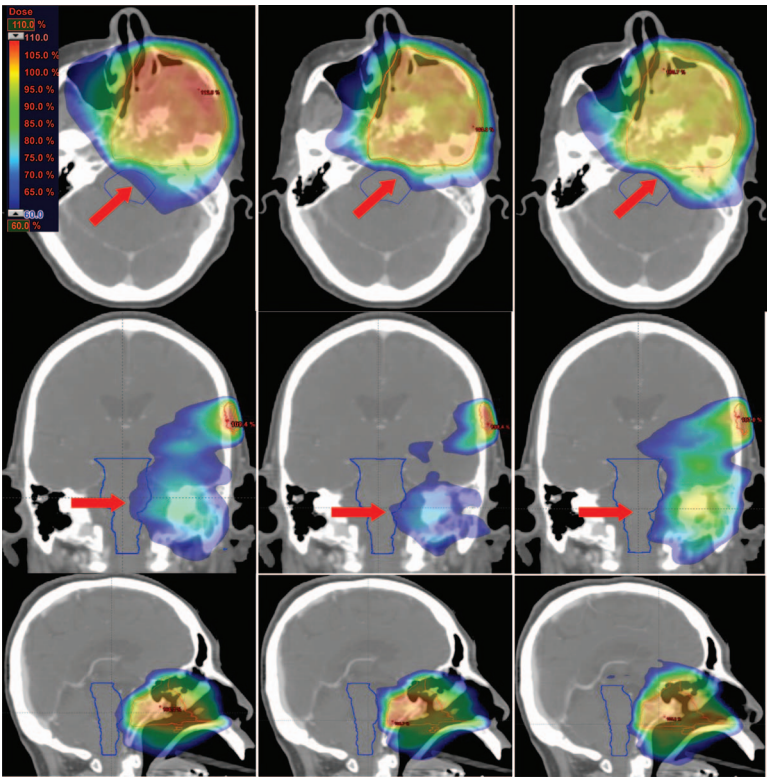
FIG. 8. Same as Fig. 7, except for a dose level of 60%–110%. Segment boosted VMAT achieves better sparing for brain stem.
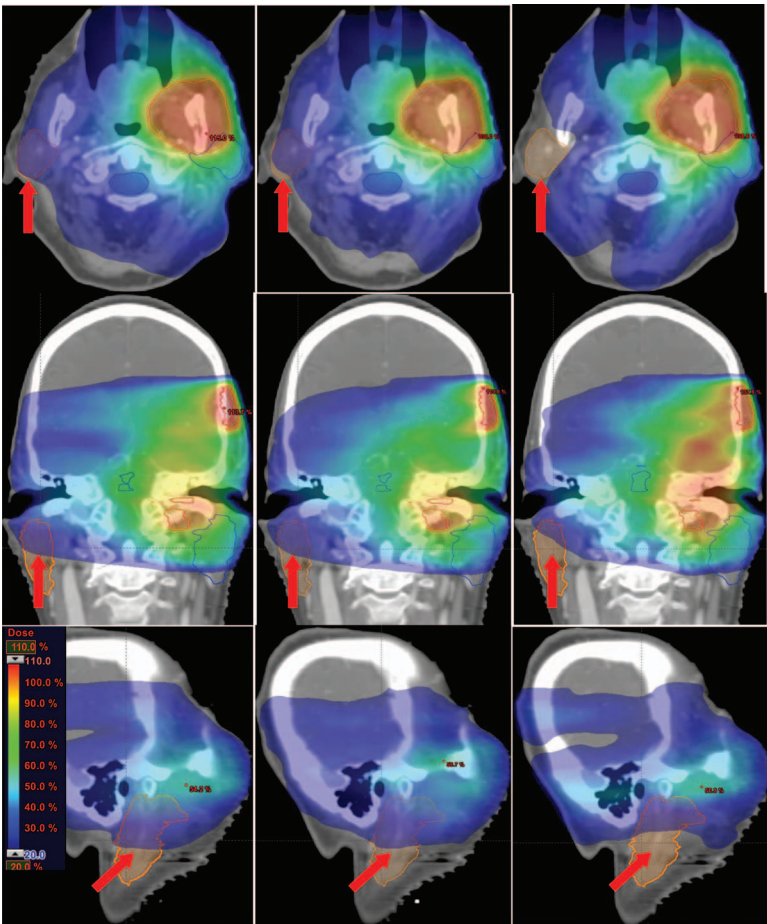

FIG. 9. Same as Fig. 7, except for a dose level of 20%–110%. Segment boosted VMAT achieves better sparing for right parotid.
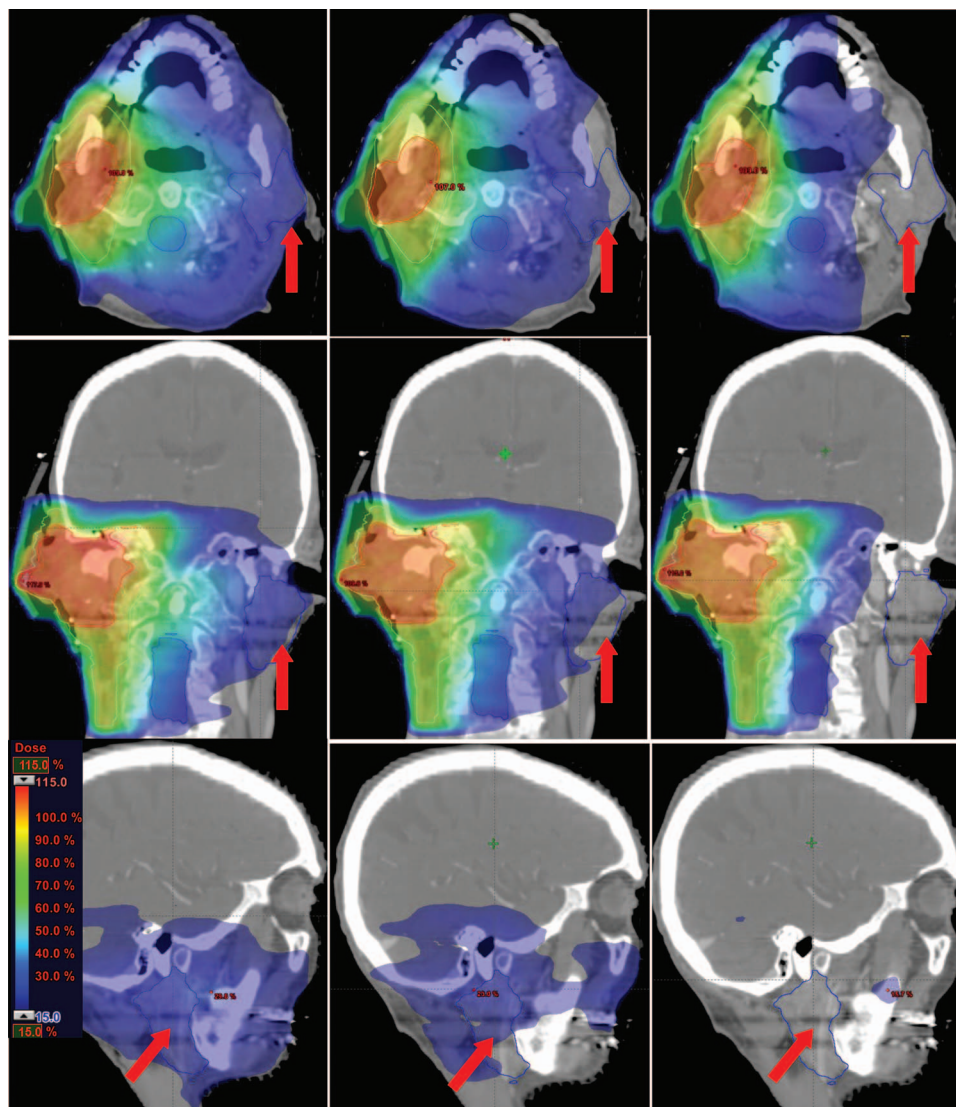
FIG. 10. Axial (top row), coronal (mid row), and sagittal (bottom row) views of the isodose distributions for three treatment plans: one-arc VMAT (left column), two-arc VMAT (mid column), and segment boosted VMAT (right column) at a dose level of 15%–115% for HN case 2. Segment boosted VMAT achieves better sparing for left parotid.

between the angular sampling and intensity modulation or, in other words, by intelligently distributing the control points.

The segmentally boost strategy presented here allows us to modulate the angular modulation differentially. Instead of imposing a uniform angular spacing between two consecutive control points, they are distributed nonuniformly to address the individual angular need for intensity modulation. We note that the specific implementation to realize segmental boost is not unique. The general goal of SPORT is to optimize the angular distribution of the control points and their apertures and weights so that the final dose distribution cannot be further improved by adding any new control points. A greedy algorithm or even an *a priori* knowledge-guided optimization[9, 10] may be implemented to accomplish this goal. As a proof of concept, we have adopted a heuristic strategy in which an initial one-arc VMAT is differentially boosted on an on-demand basis. In this process, Eq. (1) is employed as guidance for selective placement of the boosting control points. While the

number of arcs chosen for segmental boost is determined on an *ad hoc* basis in our calculation, it is possible to sequentially add the boost segments around the control point with the maximum MI.

Regarding the number of neighboring control points (the parameter K) in calculating MI, we found that the final selection of boosting angles is not very sensitive to the value of K. By definition, the MI measures the local need for intensity modulation by averaging the difference of two consecutive apertures for K control points in the vicinity of the given angle. When $K = 2$, only the two most adjacent control points are included, so on so forth. Practically, a large K involves control points that are angularly far away and thus may smear out the degree of local need for modulation. On the other hand, too small value of K will lead to noisy MI that is susceptible to local fluctuation and thus less reliable. The particular choice of $K = 10$ here is determined empirically and strikes a good balance between the two extremes.
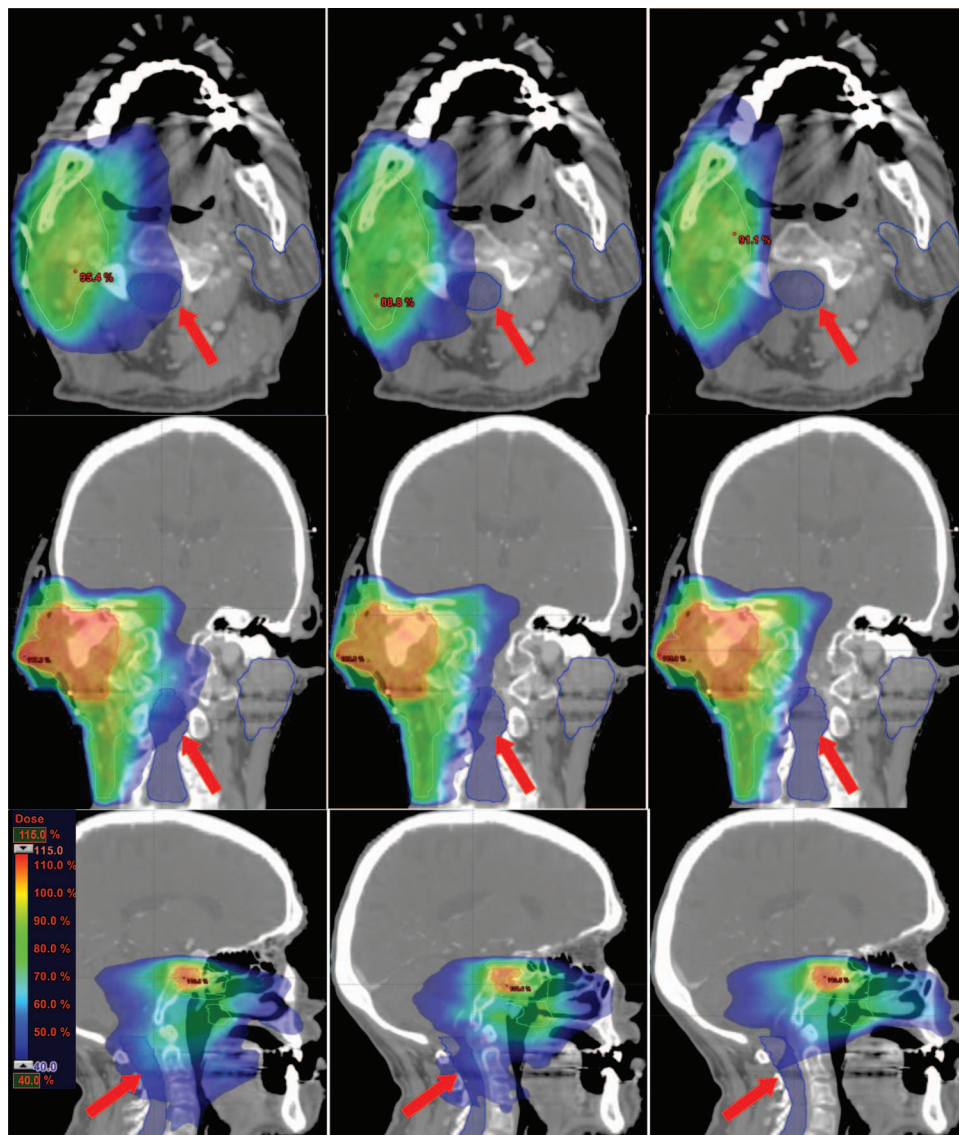
FIG. 11.   Same as Fig. 10, except for a dose level of 40%–115%. Segment boosted VMAT achieves better sparing for spinal cord.

Importantly, the delivery of the segmentally boosted VMAT plan can be accomplished in a single arc sweep by arc sequencing all the stations consisting of both original and boosting control points. Note that the gantry can even stop at certain angles to deliver multiple segments. This single-arc beam setup leads to a simplified and efficient delivery process. Table I shows the machine monitor units (MUs) required for three treatment plans in the four clinical cases. The MUs required for segmentally boosted VMAT lie between those for one-arc and two-arc VMAT. Fewer MUs also mean less head scatter and leakage radiation to the patient. As a proof of principle, the optimized SPORT plans for the HN cases have been successfully delivered on a Varian TrueBeam LINAC with custom arc sequence files.

V. CONCLUSION

A rotational arc implementation of SPORT with nonuniform angular sampling has been presented. In this strategy, the traditional one-arc VMAT is boosted differentially by adding modulated apertures on an on-demand basis. The approach overcomes the limitations of the existing treatment schemes and empowers radiation oncology discipline with a useful tool for conformal RT. The resultant dose distribution is dramatically improved as compared with the conventional VMAT. Finally, the delivery of the segmentally boosted VMAT can be accomplished by a single arc, leading to a simplified and efficient delivery process.

a)Author to whom correspondence should be addressed. Electronic mail: lei@stanford.edu; Telephone: (650) 498-7896; Fax: (650) 498-4015.

[1]G. A. Ezzell et al., "Guidance document on delivery, treatment planning, and clinical implementation of IMRT: Report of the IMRT Subcommittee of the AAPM Radiation Therapy Committee," Med. Phys. **30**(8), 2089–2115 (2003).

[2]R. Li and L. Xing, "Bridging the gap between IMRT and VMAT: Dense angularly sampled and sparse intensity modulated radiation therapy," Med. Phys. **38**(9), 4912–4919 (2011).

[3]L. Xing, M. Philips, and C. Orton, "DASSIM-RT is likely to become the method of choice over conventional IMRT and VMAT for delivery of highly conformal radiotherapy," Med. Phys. **40**(2), 020601 (3pp.) (2013).

[4]P. Zhang et al., "Optimization of collimator trajectory in volumetric modulated arc therapy: Development and evaluation for paraspinal SBRT," Int. J. Radiat. Oncol., Biol., Phys. **77**(2), 591–599 (2010).

[5]A. Niemierko, "Reporting and analyzing dose distributions: A concept of equivalent uniform dose," Med. Phys. **24**(1), 103–110 (1997).

[6]Q. Wu et al., "Optimization of intensity-modulated radiotherapy plans based on the equivalent uniform dose," Int. J. Radiat. Oncol., Biol., Phys. **52**(1), 224–235 (2002).

[7]E. Schreibmann and L. Xing, "Dose-volume based ranking of incident beam direction and its utility in facilitating IMRT beam placement," Int. J. Radiat. Oncol., Biol., Phys. **63**(2), 584–593 (2005).

[8]X. Wang et al., "Effectiveness of noncoplanar IMRT planning using a parallelized multiresolution beam angle optimization method for paranasal sinus carcinoma," Int. J. Radiat. Oncol., Biol., Phys. **63**(2), 594–601 (2005).

[9]A. Pugachev and L. Xing, "Pseudo beam's-eye-view as applied to beam orientation selection in intensity-modulated radiation therapy," Int. J. Radiat. Oncol., Biol., Phys. **51**(5), 1361–1370 (2001).

[10]A. Pugachev and L. Xing, "Incorporating prior knowledge into beam orientation optimization in IMRT," Int. J. Radiat. Oncol., Biol., Phys. **54**(5), 1565–1574 (2002).